**Marco Donnini** · **Michele Santangelo** · **Stefano Luigi Gariano** ·
**Francesco Bucci** · **Silvia Peruccacci** · **Massimiliano Alvioli** ·
**Omar Althuwaynee** · **Francesca Ardizzone** · **Cinzia Bianchi** ·
**Txomin Bornaetxea** · **Maria Teresa Brunetti** · **Mauro Cardinali** ·
**Giuseppe Esposito** · **Susanna Grita** · **Ivan Marchesini** · **Massimo Melillo** ·
**Paola Salvati** · **Mina Yazdani** · **Federica Fiorucci**

# Landslides triggered by an extraordinary rainfall event in Central Italy on September 15, 2022

**Abstract** Timely and systematic collection of landslide information after a triggering event is pivotal for the definition of landslide trends in response to climate change. On September 15, 2022, a large part of central Italy, particularly Marche and Umbria regions, was struck by an anomalous rainfall event that showed characteristics of a persistent convective system. An extraordinary cumulated rainfall of 419 mm was recorded by a rain gauge in the area in only 9 h. The rainfall triggered 1687 landslides in the area affected by the peak rainfall intensity and caused widespread flash floods and floods in the central and lower parts of the catchments. In this work, we describe the characteristics of the landslides identified during a field survey started immediately after the event. Most of the mass movements are shallow, and many are rapid (i.e., debris flows, earth flows) and widely affecting the road network. Landslide area spans from a few tens of square meters to $10^5$ m², with a median value of 87 m². Field evidence revealed diffuse residual risk conditions, being a large proportion of landslides located in the immediate vicinity of infrastructures. Besides reporting the spatial distribution of landslides triggered by an extreme rainfall event, the data collected on landslides can be used to make comparisons with the distribution of landslides in the past, validation of landslide susceptibility models, and definition of the general interaction between landslides and structures/infrastructures.

**Keywords** Extreme precipitation event · Landslide inventory · Field mapping · Climate change · Marche · Umbria

## Introduction

Despite numerous studies conducted in recent decades in the field of landslide prediction, landslides still pose a danger to people in many parts of the world (Pereira et al. 2016; Froude and Petley 2018), representing the 7th largest global killer among natural disasters (Herath and Wang 2009). A single triggering event may induce a unique slope failure or a population of landslides, in areas that can span from a single slope to thousands of square kilometers (Malamud et al. 2004; Guzzetti et al. 2012).

In Italy, Guzzetti (2000), Guzzetti et al. (2005), and Salvati et al. (2010, 2016, 2018) have analyzed historical landslides with direct human consequences on the population from 68 B.C. to 2018, finding more than 1000 fatal landslides that caused nearly 15,000 casualties. During the same period, landslides resulted in more than 200,000 homeless and evacuees.

Petley (2012) estimated that about 90% of global casualties due to slope failures can be attributed to rainfall-triggered landslides.

Moreover, landslides causing casualties are becoming more frequent in recent years, likely as a consequence of global warming (Haque et al. 2019). Indeed, global warming is expected to cause more intense and frequent rainfall events, as warmer air can hold more water than cooler air (Westra et al. 2014). Several studies investigated the temporal evolution of a series of rainfall extremes and rainfall variables at different temporal scales in Italy and the Mediterranean area. The results of these studies highlighted a general reduction in the total annual rainfall and some local trends of increasing extreme rainfall intensity for different sub-daily durations, without a clear trend at the national scale (Libertino et al. 2019; Avino et al. 2021; Chiaravalloti et al. 2022). Moreover, changes in the characteristics of landslide-triggering rainfall conditions in Europe were observed (Bezak and Mikoš, 2021).

In this context, the analysis of the rainfall conditions responsible for landslide occurrences and the identification and characterization of the landslides triggered by severe rainfall are crucial for the design of mitigation and adaptation measures.

On September 15, 2022, Central Italy (Fig. 1) was hit by an exceptional rainfall event that resulted in widespread ground effects such as floods and landslides, producing severe damage to buildings and infrastructures, as well as twelve fatalities caused by the floods downstream in different circumstances (Polaris 2022; locations of fatalities occurrence are marked with yellow dots in Fig. 1b), one missing person, about 50 injured, and more than 100 evacuees. Immediately after the event, the national government issued specific legislation to allocate funds for civil protection works and activities. By means of two resolutions of the Council of Ministers (on September 16, 2002, and November 4, 2022), the Italian national government declared a state of emergency for 12 months for the municipalities affected by the event in Marche and Umbria.

In this work, we describe the main statistical features of the rainfall event and the main characteristics (i.e., size and spatial distribution, type of failures) of the 1687 triggered landslides that were identified and mapped through an extensive reconnaissance field survey carried out in an area of ~ 550 km² across the Marche and Umbria regions.

## Study area

The area hit by the rainfall event is located in Central Italy between Marche and Umbria regions and involves a 20 km wide belt across the Northern Apennines. Overall, it encompasses about 5000 km², approximately between 12.16° Lon W to 13.36° Lon E and 43.6° Lat N and 43.2° Lat S (Fig. 1a). As shown in Fig. 1b, the rainfall event hit
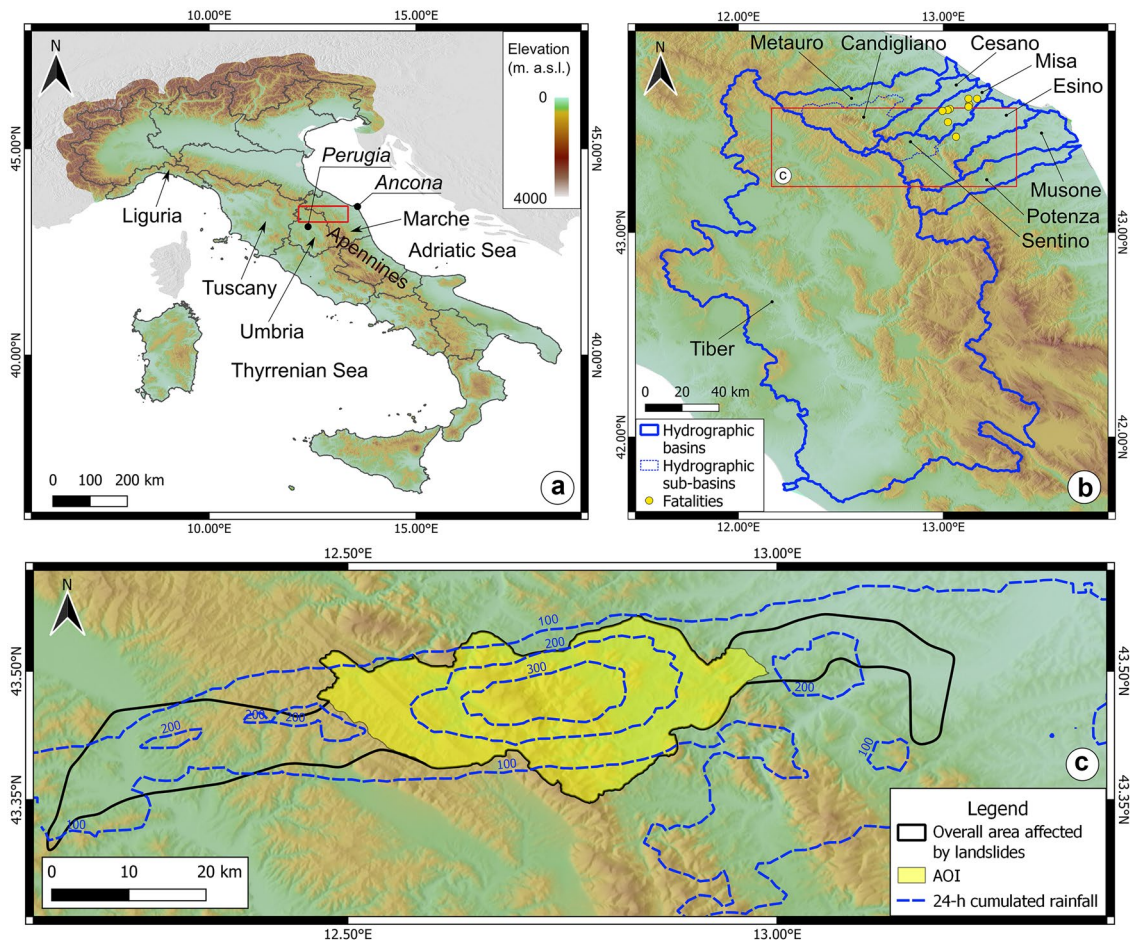
**Fig. 1  a** Index map of the affected area within the Italian peninsula, and **b** with respect to the drainage basins. **c** Overall area affected by 24-h cumulated rainfall higher than 100 mm (blue dashed lines), overall area affected by landslides (black outlined polygon); area where the event landslide inventory map was prepared (AOI, yellow polygon). EPSG:4326

an area that includes the upper portion of the Tiber River basin, the second largest Italian basin that drains into the Thyrrenian Sea, as well as the Metauro, Cesano, Misa, Esino, Musone, and Potenza river basins that drain into the Adriatic Sea. The study area encompasses anticlines and synclines pairs characterized by the general coincidence of topographic and structural relief and is centered on an NW–SE trending carbonate core punctuated by the highest mountain peaks (Mt. Nerone, 1525 m a.s.l.; Mt. Catria, 1701 m a.s.l; and Mt. Cucco, 1566 m a.s.l.). These anticlinal ridges affect the Mesozoic-Cenozoic rocks of the Umbria-Marche platform-to-pelagic sequence, consisting of carbonate rocks including massive and stratified limestones, well-bedded marly limestones, and marls. The structures consist of a large asymmetric fold, with steep western limbs and nearly vertical to overturned eastern limbs, with a gently rounded to flat top. The overturned eastern limbs of these structures link with overturned, east-verging synclines and face eastward the Neogene marly terrains of the Marche hills. Instead, the western limbs of these structures dip under younger siliciclastic (i.e., sandstone, mud-stone, and greywacke) sedimentary rocks pertaining to the Miocene Marnoso Arenacea Formation, in turn arranged in east-verging fold and thrust and exposed in a more internal NW–SE trending relief approaching 900 m of elevation. These NW–SE trending reliefs cover most of the study area and are separated by syncline valleys where clastic rocks and alluvial deposits fill narrow and elongated fluvial-alluvial plains and seismically active intermontane basins (Mirabella et al. 2018). Due to the great variability of the relief and the generally significant slopes, erosion does not allow the formation of very deep soils in the study area. Especially where carbonates prevail, mountainous terrain and carbonate-derived debris slopes are common, and thin to moderately deep granular soils develop, with a loamy texture and a frequent skeleton. On the other hand, where mixed lithologies (e.g., turbiditic sequences) prevail, as in the hilly terrains and farmlands surrounding Mt. Catria, the soil's texture presents a certain variability due to the alternation of layers with different lithologies, with finer earth grains derived from marls and pelites.

The area is mainly devoted to rural use, being mainly composed of agricultural and forest/semi-natural areas, as shown by the 2021 Corine Land Cover (Corine Land Cover 2021). The most populated urban settlements are the towns of Città di Castello, Gubbio, and Jesi (between 30,000 and 40,000 inhabitants), as well as Cagli and Cantiano (with less than 10,000 inhabitants).

**Table 1** Values of the cumulated rainfall (E) and duration (D) of the event, measured by eight rain gauges in the area. Values of maximum cumulated rainfall in 1 h ($E_{max1h}$) are also reported. The location of the rain gauges is shown in Fig. 2a

| Name | Lat (° N) | Lon (° E) | E (mm) | D (h) | $E_{max1h}$ (mm) |
|---|---|---|---|---|---|
| Cantiano | 43.467068 | 12.640526 | 419.0 | 9 | 101.4 |
| Monte Acuto | 43.477711 | 12.691960 | 384.0 | 9 | 90.4 |
| Fonte Avellana | 43.471085 | 12.726417 | 373.2 | 10 | 86.4 |
| Cingoli | 43.362240 | 13.192330 | 247.0 | 10 | 88.8 |
| Colle | 43.534794 | 13.056502 | 204.0 | 9 | 74.0 |
| San Benedetto Vecchio | 43.436667 | 12.463889 | 195.0 | 8 | 44.4 |
| Scheggia | 43.406490 | 12.658760 | 187.4 | 7 | 53.8 |
| Pieve di Saddi | 43.426944 | 12.361667 | 176.8 | 10 | 59.6 |

The climate in the area is typical of the Apennines range, characterized by a main maximum rainfall period at the end of autumn, a main minimum rainfall period in summer, and a minor minimum at the end of winter. The mean annual temperature recorded in the Apennines ranges from 10.0 to 14.4 °C, with a mean temperature of the coldest month from 4.0 to 5.9 °C and 3 months with a mean temperature larger than 20.0 °C. Generally, rainfall reaches values of more than 1500 mm per year on the slopes that are exposed to the dominant western winds (Fratianni and Acquaotta 2017). In the study area, the mean annual precipitation and temperature in 30 years (1991–2020) are about 950 mm and 13 °C, respectively, according to the SCIA database of the Italian Institute of Protection and Environmental Research, ISPRA (Desiato et al. 2007, 2014).

Due to its lithological, morphological, seismic, and climatic setting, landslides and erosional processes are abundant in the area (Santangelo et al. 2021). In the Umbria and Marche regions, landslides are commonly triggered by rapid snow melt (Cardinali et al. 2000), earthquakes (Esposito et al. 2000; Antonini et al. 2002), and, most commonly, intense and prolonged rainfall (Guzzetti 2000; Guzzetti et al. 2002, 2003; Floris and Veneri 2004; Cardinali et al. 2006; Fiorucci et al. 2011; Peruccacci et al. 2012; Donnini et al. 2017; Gariano et al. 2021).

Preliminary field surveys, carried out in the immediate aftermath of the rainfall event, allowed estimating that the overall area affected by landslides exceeded 970 km² (black outlined polygon in Fig. 1c). It was then carried out a systematic reconnaissance field survey to prepare an event landslide inventory map (Guzzetti et al. 2012) for a smaller area (yellow polygon in Fig. 1c) that includes a large neighborhood of the area that recorded the highest rainfall intensity, for a total area of about 550 km², henceforth referred to as area of interest (AOI).

### Event description

#### Rainfall event

The exceptional rainfall event that hit a portion of Central Italy on September 15, 2022, showed a "self-regenerating" storm structure, i.e., a convective system persisting over the same area for several hours (Nuissier et al. 2008; Ducrocq et al. 2014; Pensieri et al. 2018), and exhibiting a typical "V" shaped geographical pattern (Scofield 1985; Duffourg and Ducrocq 2011). Key roles in the development of persistent convective systems are played on one side by the stationary convergence between two air masses with sharply contrasting temperature and water vapor content and on the other side by morphological relief (Pensieri et al. 2018). Such phenomena are well known in Italy, even though most commonly observed in the area of northern Tuscany and Liguria (Pensieri et al. 2018; Mazzoglio et al. 2022), such as during the events of Genoa (2011 and 2014), Cinque Terre (2011), Livorno (2017), and Val Bormida (2021), which have caused relevant damages to people and infrastructures (Fiori et al. 2014; Buzzi et al. 2014; Ricciardelli et al. 2018; Faccini et al. 2018; https://polaris.irpi.cnr.it/).

During the late morning of September 15, storm systems formed over the Thyrrenian side of the Italian peninsula. Those storm systems migrated eastward and generated additional storm cells that progressively involved Tuscany and reached Umbria and Marche regions in the afternoon where they assumed the characteristics of a stationary self-regenerating system which caused an increase in the rainfall intensity for a period of 6–7 h. As shown in Table 1 and in Fig. 2, the highest cumulated rainfall value (E) was recorded at the rain gauge in Cantiano with 419 mm for a duration (D) of 9 h (starting at 3:00 p.m.). More in detail, thanks to the availability of 15-min measurements for the Cantiano rain gauge, we could estimate a more precise duration of the event, i.e., 8 h and 15 min, with a significant peak of 39.0 mm in 15 min (6:15 to 6:30 p.m.). Remarkably, the same rain gauge measured 256.6 mm in 3 h (4:00 to 7:00 p.m.) and 101.4 mm in 1 h ($E_{max1h}$ in Table 1). However, given that the minimum common resolution for all the available rain gauges is 1 h, for the sake of homogeneity, all the following analyses were conducted at an hourly temporal resolution. Inspection of Table 1 and Fig. 2a reveals that the exceptionally high cumulated rainfall value (E) was not isolated, as more than 300 mm were measured in Monte Acuto and Fonte Avellana rain gauges and more than 200 in Cingoli and Colle rain gauges (Fig. 2a). Additionally, radar data provided by the Italian Department of Civil Protection[1] estimated a 24-h (starting on September

---

[1] STR1 product, corrected with ground-based measurements, https://mappe.protezionecivile.gov.it/it/mappe-rischi/piattaforma-radar
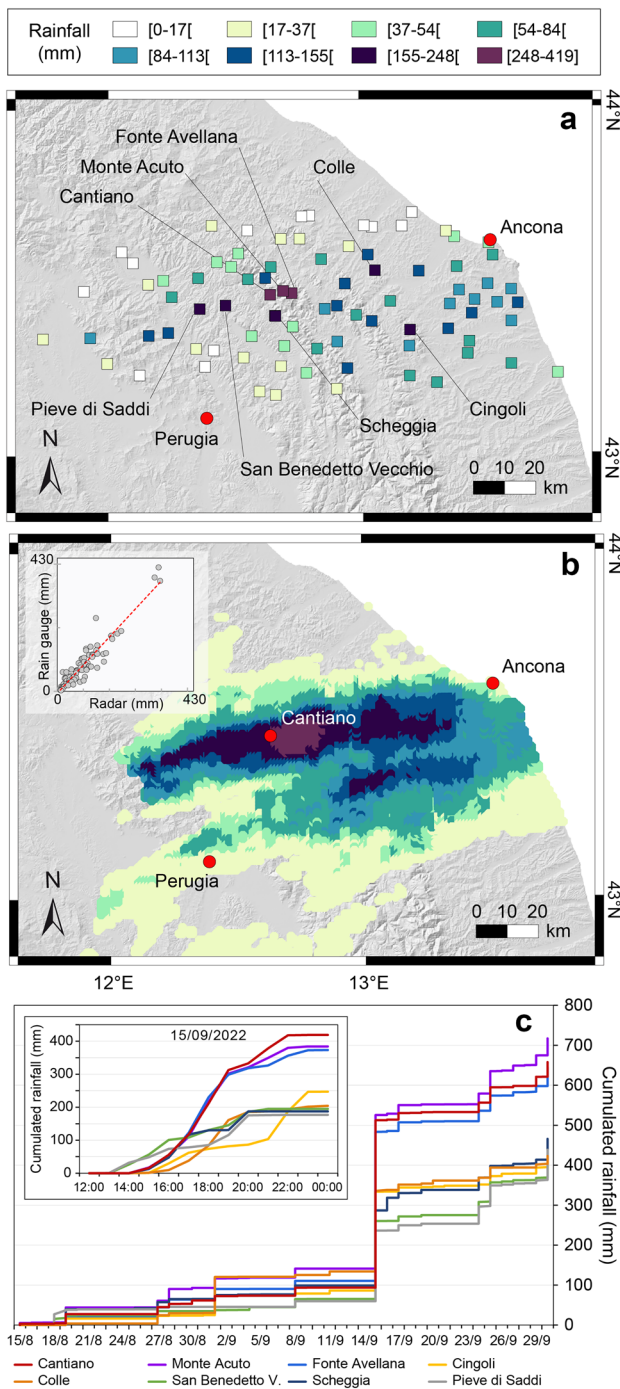
**Fig. 2 a** Cumulated rainfall measured by the 85 rain gauges located in the affected area in the same time interval; the eight stations that measured the highest cumulated rainfall values are labeled). **b** Map showing the 24-h cumulated rainfall estimated by Civil Protection radars (1-km cells); the location of Cantiano and the regional capitals of Marche and Umbria (Ancona and Perugia) are shown; the inset shows the correlation among the series ($R^2 = 0.888$). Classes in the legend made by Jenks natural breaks. EPSG 4326. **c** Cumulated rainfall from 30 days before to 15 days after September 15, 2022; rainfall measurements from eight rain gauges are listed in Table 1. The inset shows the cumulated rainfall values for the September 15 event

15 at 06:00) cumulated rainfall exceeding 100 mm over an area greater than 1500 km² (Fig. 2b). Figure 2a shows the cumulated rainfall measured by the 85 available rain gauges in the area during the same time interval. The scatterplot in Fig. 2b shows a general good agreement between rain gauge measurements and radar estimates at the same locations ($R^2 = 0.888$).

Figure 2c shows the rainfall cumulated from 30 days before to 15 days after the main rainfall event, measured by eight rain gauges listed in Table 1. No significant rainfall was recorded in the 30-day period preceding the event: around 100 mm (141 at Monte Acuto station) were measured between August 15 and in September 1, and only a few mm in the first 15 days of September (e.g., less than 20 mm in 15 days recorded by the Cantiano station). This suggests dry soil conditions in the 15-day period preceding the event, also given the summer season. The inset in Fig. 2c shows the cumulated rainfall values from 2 p.m. to midnight of September 15, allowing an estimation of the main pattern of the rainfall event. The rain gauges located westerly (e.g., San Benedetto Vecchio and Pieve di Saddi) started recording the rain more than 2 h earlier than the station located to the east (e.g., Cingoli and Colle). However, those gauges measured much lower values than the Cantiano, Monte Acuto, and Fonte Avellana stations, located in the area more affected by the rainfall.

The intense rainfall induced a rapid rise in hydrometric levels in the basins of the central mountain belt of Marche region causing widespread flooding. The most affected basins were those of Candigliano (a sub-basin of Metauro), Cesano, Misa, Sentino (a sub-basin of Esino), and Musone rivers (Fig. 1b). During the rainfall event, some hydrometric stations of the regional network were damaged by the flood or experienced transmission problems at peak rainfall intensity (Regione Marche - Centro Funzionale Regionale 2022).

Considering the historical record of the Cantiano rain gauge, the September 15, 2022 event recorded about one-third of the overall annual rainfall, as the average annual rainfall over the last 30 years (1991–2021) is 1268 mm (1273 mm if the entire 71-year time series is considered, http://www.scia.isprambiente.it/wwwrootscia/Home_new.html). Table 2 compares the average, median, and maximum values of the hourly maxima (at 1, 3, 6, 12, and 24 h) recorded in the period 1950–2021 at the Cantiano rain gauge, to the values recorded during the September 15, 2022 event. Rainfall values recorded in the event are far above historical maxima for each duration, especially the 3-h and 6-h cumulated rainfall values, more than 250% higher than the historical maxima. Such figures show that this rainfall event is extremely rare for this area.

**Landslide inventory**

The mapping activity involved 19 people and lasted 20 days. The reconnaissance field survey was carried out by teams of at least three experts, one of which with decadal experience in landslide mapping. Each team was assigned a parcel of the total area of interest to optimize the mapping activities. The teams drove along the main and secondary roads stopping at every landslide or scenery point. Each landslide was mapped in the field using GoogleEarth as the base map, and related pictures were taken. To

**Table 2** Average, median, and maximum values of the hourly maxima (at 1, 3, 6, 12, and 24 h) recorded in the period 1950–2021 at the Cantiano rain gauge, compared to the values recorded during the September 15, 2022 rainfall event. Dates of the historical maxima and percentages of increase (Δmax) in the current event are also reported in brackets

| D (h) | Hourly maxima (mm) | | | |
| --- | --- | --- | --- | --- |
| | Average 1950–2021 | Median 1950–2021 | Max 1950–2021 | September 15, 2022 (Δmax, %) |
| 1 | 26.4 | 23.5 | 63.6 [June 25, 2017] | 101.4 (+59%) |
| 3 | 37.6 | 35.8 | 84.0 [September 6, 1984] | 256.6 (+205%) |
| 6 | 48.8 | 45.3 | 100.0 [September 6, 1984] | 384.0 (+284%) |
| 12 | 66.6 | 64.0 | 120.2 [May 12, 2019] | 419.0 (+249%) |
| 24 | 89.0 | 81.0 | 173.6 [November 10, 2013] | 419.0 (+141%) |

prepare the inventory, field activity was not supported by UAV inspections or any available remote sensing imagery, or interviews to the local residents.

Our inventory reports 1687 landslides, and 1243 landslides were originally mapped as polygons, whereas the remaining 444 landslides, whose area was estimated in only a few square meters, were directly mapped as points (i.e., without information on landslide area). For readability purposes, all figures representing the landslide distribution in this paper adopt points as representing features.

Following the classification scheme by Hungr et al. (2014), each landslide was classified according to the type of material involved (rock, debris, or earth) and to the type of movement (slide, slide-flow, flow, and fall). The inventory is described in detail by Santangelo et al. (2023a) and the dataset is publicly available (Santangelo et al., 2023b). For readability purposes, all figures representing the landslide distribution in this paper adopt points as representing features.

Table 3 reports a summary of landslide count ($N_L$) and total area ($A_L$) based on the type of movement and material involved. It should be noted that the landslide area is slightly underestimated because 444 landslides were originally mapped as points. Figure 3 shows some representative examples of the different landslides triggered in the AOI. Considering landslide material, 60% involve earth (Fig. 3c, h), 39% debris, (Fig. 3a, b), and 1% rock. Regarding the type of movement, 65% were classified as slides, 21% as flows, 13% as slide-flows, and 1% as falls. Overall, the most common landslide type is earth slide (49% of the total inventory, Fig. 3c, h), followed by debris flow (17%, Fig. 3e, f) and debris slide (13%, Fig. 3d).

Slide-type landslides (Fig. 3c, d, h) present a well-defined scarp and are most commonly translational. The slide deposit is convex, and the material is characterized by low mobility.

Earth slides (Fig. 3c, h) are generally shallow as opposed to debris slides, locally slightly deeper. Occasionally, slide movements involved also rock material. Slide-flows (Fig. 3a, b, g) show the characteristics of slides (most commonly translational) in the escarpment area, whereas the deposit is elongated and sometimes branched due to the high water content of the mobilized material so that even subtle convexities of the topographic surface act as local divides. Material involved in this type of movement is debris (Fig. 3a, b) and earth (Fig. 3c, h). Flow-like landslides (Fig. 3e, f) involve the movement of material down a slope in the form of a fluid, and the shape of the deposit is often a characteristic fan. In this event, flows involved mainly earth and debris (Fig. 3e, f). Fall is the least represented type of movement in the inventory (1%), and the material involved is rock. Rockfall deposits are usually made of single blocks or talus at the base of the slopes.

Figures 4a, b show the distribution of landslide number density ($D_N$) and size density ($D_S$) in the AOI. Inspection of the figures reveals a spatial mismatch between the maxima of $D_N$ and $D_S$, the former located in the eastern sector, the latter in the central sector. We interpret the evidence that larger landslides occurred in the central part as opposed to the more numerous but smaller failures in the eastern sector mainly as the combined effect of morphology and land use, as the central sector is characterized by the highest relative relief inducing larger and longer slopes, which are almost entirely wooded, thus preventing small failures. In general, however,

**Table 3** Summary of the number and total area of landslide types represented in the event landslide inventory map

| | Fall | | Flow | | Slide-flow | | Slide | | Total | |
| --- | --- | --- | --- | --- | --- | --- | --- | --- | --- | --- |
| | $N_L$ | $A_L$ (m²) | $N_L$ | $A_L$ (m²) | $N_L$ | $A_L$ (m²) | $N_L$ | $A_L$ (m²) | $N_L$ | $A_L$ (m²) |
| Rock | 18 | $5.1 \times 10^3$ | - | - | - | - | 6 | $6.9 \times 10^3$ | 24 | $1.2 \times 10^4$ |
| Debris | - | - | 304 | $6.0 \times 10^5$ | 132 | $1.9 \times 10^5$ | 232 | $1.1 \times 10^5$ | 668 | $9.0 \times 10^5$ |
| Earth | - | - | 65 | $2.2 \times 10^4$ | 88 | $4.9 \times 10^4$ | 842 | $1.4 \times 10^5$ | 995 | $2.1 \times 10^5$ |
| Total | 18 | $5.1 \times 10^3$ | 369 | $6.2 \times 10^5$ | 220 | $2.4 \times 10^5$ | 1080 | $2.5 \times 10^5$ | 1687 | $1.1 \times 10^6$ |

$N_L$ number of landslides, $A_L$ landslide area in square meters
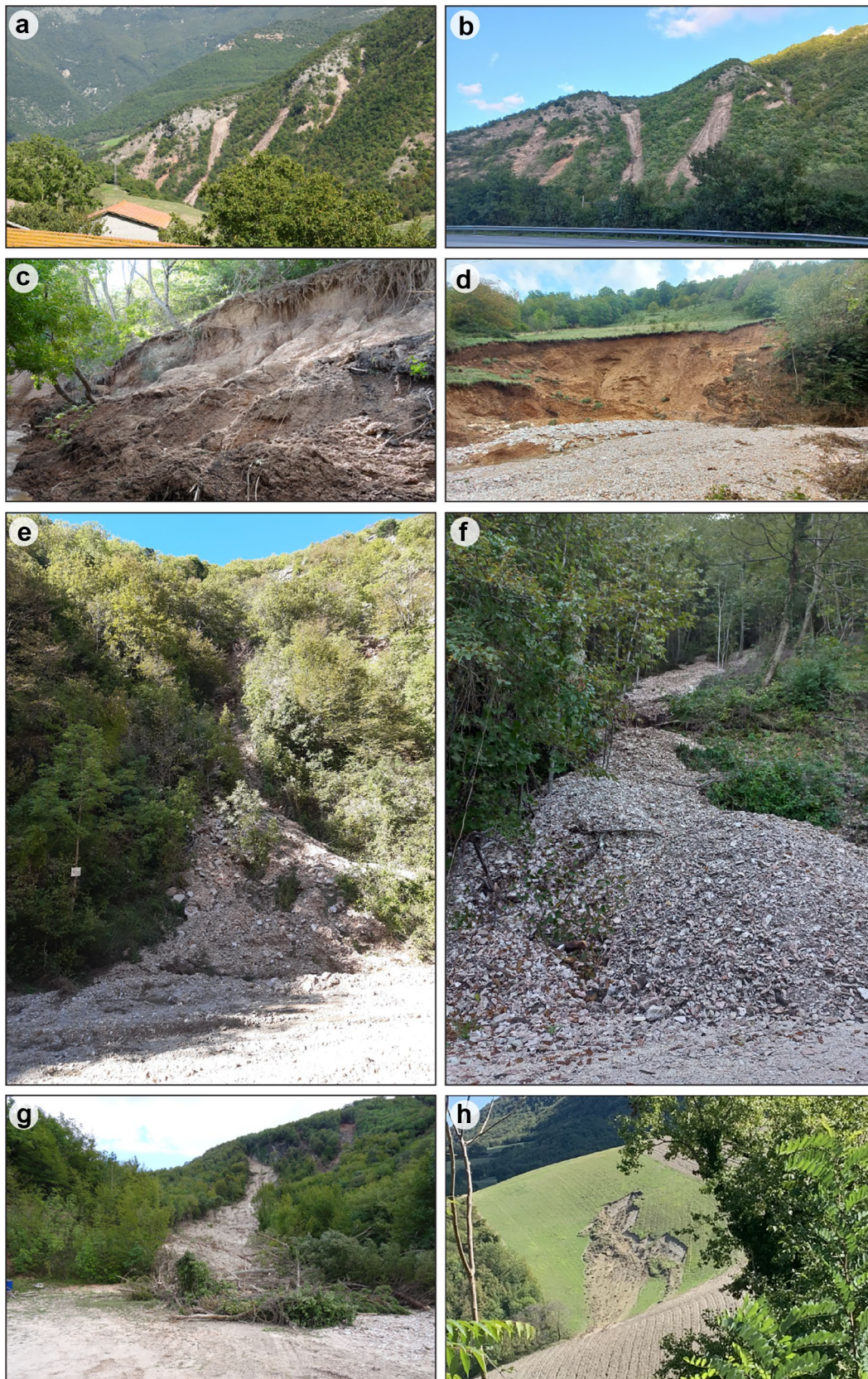
**Fig. 3** Examples of landslides observed in the area. **a**, **b** Debris and earth slide-flows; **c** earth slide; **d** debris slide; **e**, **f** debris flow; **g** debris slide-flow; **h** earth slide
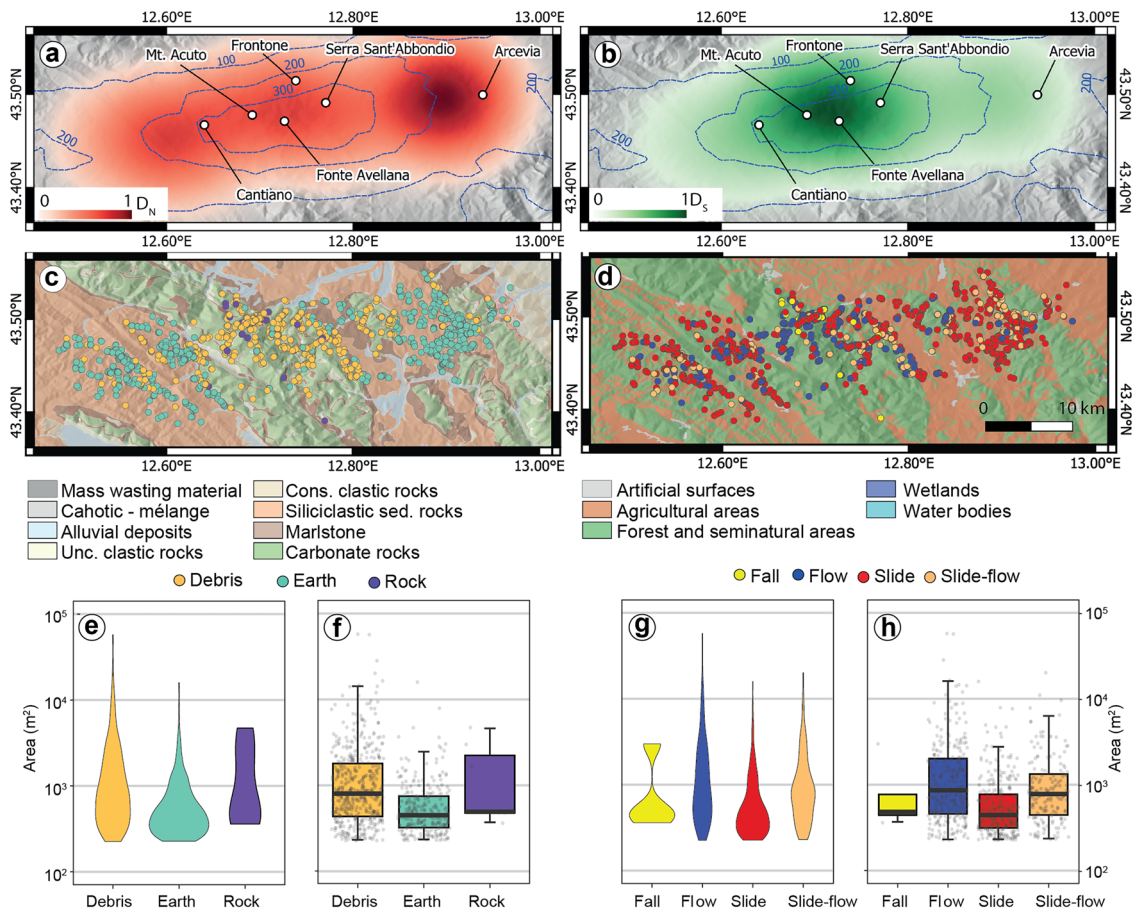
**Fig. 4** **a** Relative density of landslide number ($D_N$) and **b** of landslide size ($D_S$), computed through kernel density analysis in a GIS environment. **c** Landslide material compared to lithology. **d** Landslide type of movements compared to land cover of the AOI. **e** Violin plots and **f** boxplots of landslide area based on landslide material; **g** violin plots and **h** boxplots of landslide area based on landslide type of movement

both $D_N$ and $D_S$ maps well match the main plume of the rainfall event, corresponding to 24-h cumulated rainfall values greater than 155 mm (Fig. 2b), with $D_S$ maximum perfectly matching the rainfall intensity peak (> 248 mm).

In Fig. 4c, d, all the event landsides are represented as points. In detail, Fig. 4c shows the distribution of landslide material superimposed on the lithological map of Bucci et al. (2022), while in Fig. 4d, the type of movement is overlaid to land cover (Corine Land Cover 2021). Combined inspection of Fig. 4c, d reveals that the type of material involved is controlled by lithology, whereas the type of movement appears related to land cover. In particular, 94% of falls and 75% of flows occurred in forest and semi-natural areas, while 67% of slides occurred in agricultural areas, and only 31% in forest and semi-natural areas. Complex movements, such as slide-flows (Fig. 3a, b), appear less correlated to land cover, although they are more numerous in forest and semi-natural areas (59%) than in agricultural areas (40%). Furthermore, the majority of debris flows occurred within carbonate rocks (61%), followed by marlstones (19%) and siliciclastic rocks (12%). Similarly, rock falls occurred predominantly in carbonate rocks (79%) and subordinately in marlstones (21%). On the other hand, the majority of earth

flows occurred within siliciclastic rocks (75%) and only to a minor extent in marlstones (14%).

Landslide size is generally small (median smaller than $10^3$ m²), with the largest failures not reaching $10^5$ m². In general, landslides involving debris are larger than those involving earth or rock (Fig. 4e, f); considering the type of movement, failures showing at least a component of flow are larger than the others (Fig. 4g, h). Interaction between landslides and structures/infrastructures was relevant (Fig. 5).

Many national and local roads were interrupted, mostly by earth and rock slides (e.g., Fig. 5a); national and local railways were interrupted at several points; extensive damage was registered to structures and infrastructures (e.g., Fig. 5e, f). Furthermore, field evidence revealed that a vast proportion of landslides occurred in the immediate vicinity of roads, mostly affecting road embankments (e.g., Fig. 5b, f, h) and that a large number of landslides initiated within natural and semi-natural areas and hit the road network and, locally, affected houses and activities (e.g., Fig. 5e, g).

Figure 6 shows the cumulative distribution of landslide count ($N_L$, Fig. 6a) and area ($A_L$, Fig. 6b) based on distance to road ($D_R$), computed for any road considering the landslide centroids,

**Fig. 5** Examples of landslides that hit roads and structures. **a** Rock slide on the SS3 national road, Scheggia municipality; **b, c, h, g** earth slide; **d** rock fall; **e** debris flow; **f** rock slide
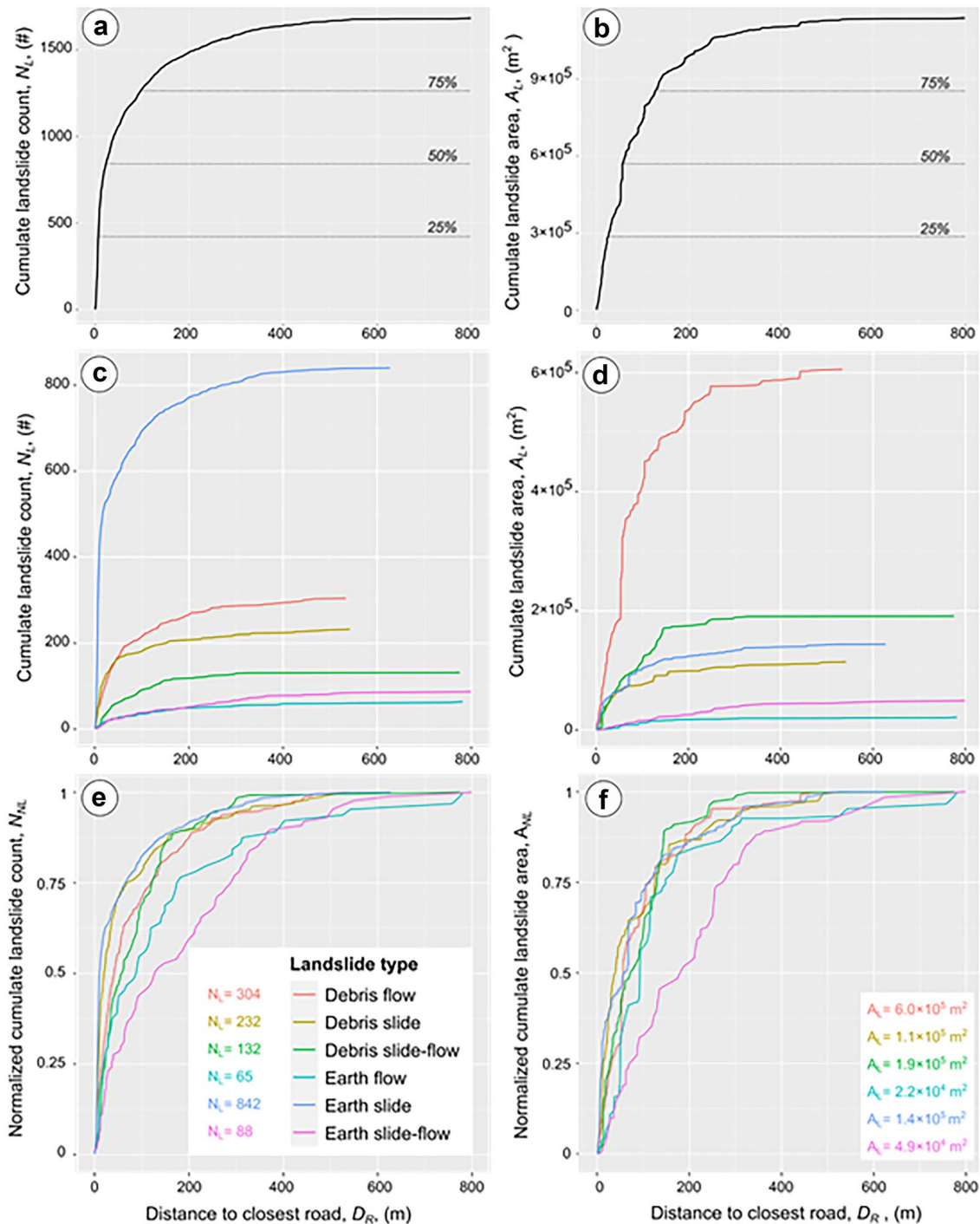
**Fig. 6** Cumulative landslide count ($N_L$) and area ($A_L$) with respect to distance to road ($D_R$): **a** and **b** for all landslides; **c** and **d** grouped by landslide types; **e** and **f** grouped by landslide types and normalized by count ($N_{NL}$) and total area ($A_{NL}$) for specific landslide type. Rockfalls and rock slides were excluded from **c** to **f** as they are not statistically significant. In **a** and **b**, dashed lines indicate reference percentage values for cumulative landslide count and area

regardless of whether or not it was used during the survey. The plot in Fig. 6a suggests that ~ 1000 landslides (~ 60% of the total) occurred within 50 m from the roads and ~ 750 (~ 45% of the total) within 20 m. Considering landslide area, ~ 50% of the total landslide area occurred within 50 m (~ 15% within 20 m) from a road.

If landslide type is considered, data show that earth slides are the most represented landslide type in the immediate vicinity of roads (~ 80% within 50 m and ~ 60% within 20 m, Fig. 6c, e). On the other hand, if landslide area is considered, debris flows show the largest total area (Fig. 6d, f) close to the road network compared to
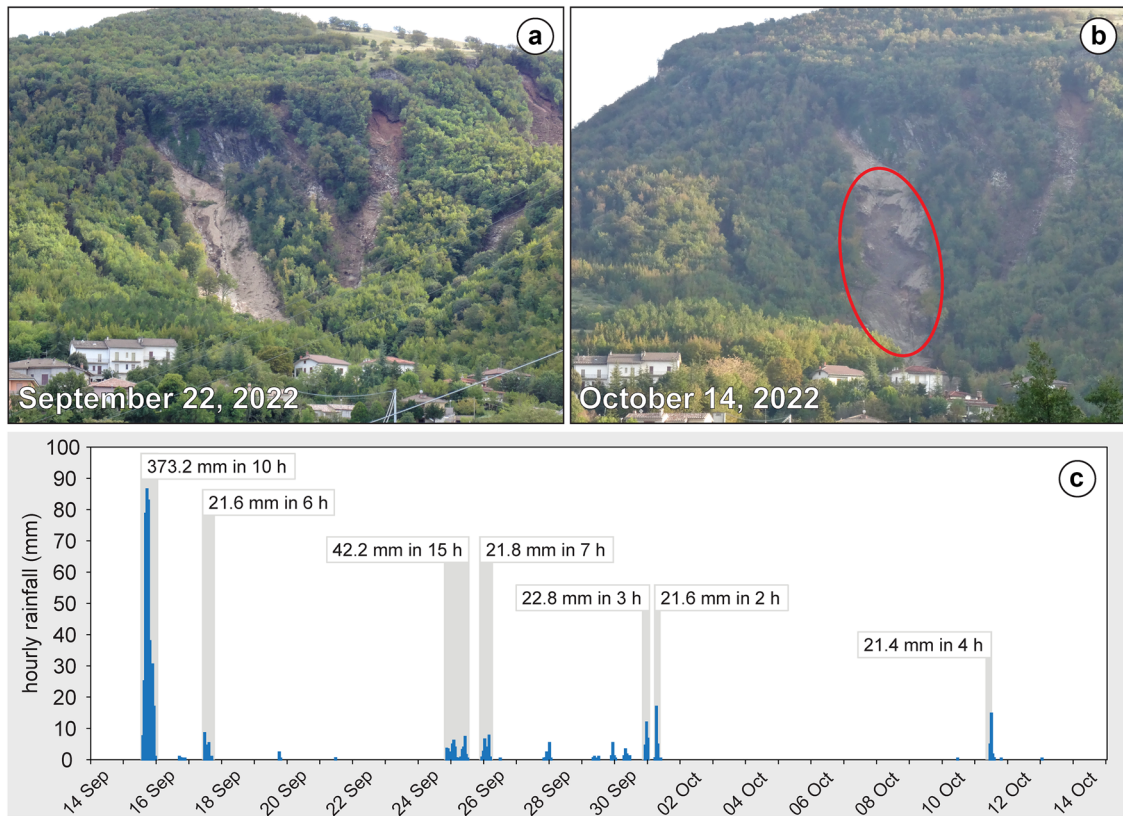
**Fig. 7** Debris slide-flow that affected Leccia village (Serra Sant'Abbondio municipality). The two photos (**a**, **b**) show modifications of the landslide in the two surveying dates. The bar chart (**c**) shows the hourly rainfall measured by the closest rain gauge (Fonte Avellana) between September 14, and October 14, 2022. Rainfall events with cumulated rainfall greater than 20 mm are highlighted in grey and labeled
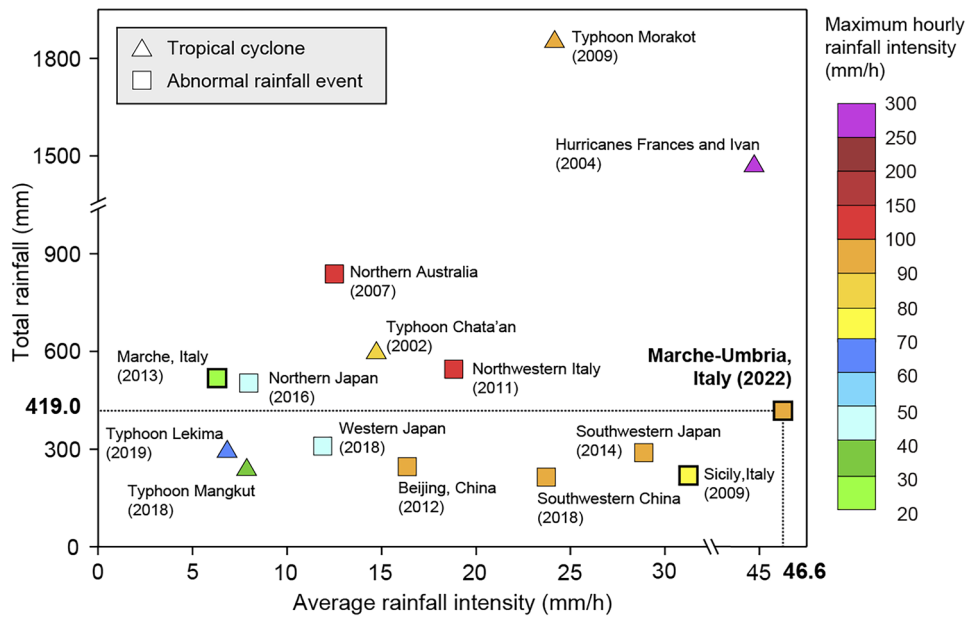


**Fig. 8** Comparison of the rainfall parameters of the Marche-Umbria event and other severe, regional-scale rainfall events worldwide. Modified from (Liang et al. 2022). Squares with thick border are the Marche-Umbria 2022 event and Marche 2013 and Sicily 2009 events

any other landslide type (~ $2 \times 10^5$ m² within 50 m and ~ $1 \times 10^5$ m² within 20 m). On the other hand, the distribution of both $N_L$ and $A_L$ of earth flows and earth slide-flows in Fig. 6c, d show the lowest gradient, which reveals that such landslides are less abundant close to the road network and that they are among the smallest failures in the inventory (Table 3).

## Discussion and conclusions

The landslide inventory presented in this work represents a first evaluation of the ground effects of an exceptional rainfall event, which intensity had never been recorded in the available rainfall time series of this area in Central Italy.

As usually happens when preparing event landslide inventories through reconnaissance field mapping, if on one side they allow mapping with extreme detail even metric failures under the trees canopy, on the other side, they can be affected by some incompleteness due to accessibility and/or visibility constrains (Bornaetxea et al. 2022). Hence, particular caution is recommended in the interpretation of local clusters (or local absences) of landslides (Fig. 4a), which could result from partial biases linked to road density/accessibility at the time of the survey. However, despite a degree of incompleteness, we maintain that the 1687 mapped landslides are representative of the overall landslide occurrence in the study area, in terms of density, size, and type.

The aforementioned characteristics of the event landslide inventory have a direct influence on the use of such information. In particular, the inventory can be used to make comparisons with the distribution of landslides in the past (i.e., geomorphological historical inventories and multi-temporal inventories sensu Guzzetti et al. 2012), validation of landslide susceptibility models (Reichenbach et al. 2018), and definition of the general interaction between landslides and structures/infrastructures (Donnini et al. 2017).

Further inspection of the cumulative distribution of landslide count and area based on distance to road show that all the curves, regardless of landslide type, are convex, hence the proportion of the number of failures and their area is greater close to the road network, both in terms of absolute number/area (Fig. 6c, d) or their relative proportion (Fig. 6e, f).

For instance, earth slides are extremely clustered close to the road network (i.e., steep curve for low $D_R$ values, Fig. 6c, e); on the other hand, earth slides are less represented in terms of their area (Fig. 6d, f). Such evidence confirms the field evidence that the small area of earth slides close to the road network is controlled by the limited size of the affected road embankments, promoted by the high local slope and the reduced cohesion of the road embankment material (Fig. 5b).

Furthermore, debris flows are less abundant within a few tens of meters from the road network compared to earth slides (Fig. 6c), but their cumulative area is the largest (Fig. 6d). This evidence indicates that, locally, debris flows of considerable size have already impacted the road network (Fig. 5e) or are in the immediate vicinity of roads. Field evidence suggests that all debris flows initiated on natural or semi-natural slopes and that roads did not exert a control on their occurrence.

Figure 7 shows a debris slide-flow occurred in Leccia village (43°28′49.00″N, 12°46′46.19″E) that underwent a relevant remobilization between September 22 and October 14, 2022 (Fig. 7a, b). Figure 7c shows the hourly rainfall measured by the closest rain gauge (Fonte Avellana, 5 km). Arguably, due to the residual geotechnical conditions of this slope, the remobilization of the debris slide-flow was triggered by rainfall characterized by far lower peak hour intensity (< 17 mm) or maximum 24-h (< 51 mm) cumulative values compared to the first triggering event (373.2 mm in 10 h, with 86.4 mm hourly peak, Table 1).

Inspection of Fig. 7c shows that the rainfall events responsible for the extensive landslide remobilization are far smaller than the rainfall event that triggered it. This evidence suggests that after severe rainfall events, even minor rainfall events might cause extensive remobilization of landslides due to residual/metastable conditions. Local residual risk conditions should therefore be considered by land administrators when issuing geo-hydrological alerts based on weather forecast.

Figure 8 shows how the Marche-Umbria event ranks in the analysis performed by Liang et al. (2022) along with another rainfall event that hit the Marche region in 2013 (Donnini et al. 2017) and a rainfall event that hit Sicily in 2009 (Ardizzone et al. 2012). In particular, the Marche-Umbria event is located in the lower-right corner of the scatter plot. Considering the values measured by the Cantiano rain gauge, the total cumulated rainfall of this event is higher than seven large events that occurred worldwide, the maximum hourly rainfall lies above the center of the scale (orange color), and the average rainfall intensity is the highest in the plot. Comparing the rainfall events that hit the Marche region in 2022 and 2013, it can be observed that the total rainfall values are comparable, while the average rainfall intensity is very different: 499 mm in 84 h in 2013 and 419 mm in 9 h in 2022. The September 15, 2022 event shows an extraordinary average rainfall intensity for the region, and apparently, it is relevant also at the global scale.

Given the type of landslides that were observed in the described event, we can assert that the vast majority of landslides are shallow and most of them are rapid moving (i.e., show at least a flow component). Such an evidence is in agreement to other events that occurred worldwide (Ardizzone et al. 2012; Alvioli et al. 2018; Santangelo et al. 2022) and suggests that exceptional/extreme rainfall events trigger mostly rapid moving landslides, mainly due to a high water availability inducing a rapid increase in water content and pore pressure and loss of matric suction in the first soil horizons, not necessarily linked to peculiar flow accumulation patterns. According to the climate change scenarios, future rainfall patterns may trigger even more rapid landslides (Gariano and Guzzetti 2016), the deadliest landslide type (Mondini et al. 2014; Alvioli et al. 2018). In general, more effort is needed to collect the effects of climatic extremes (such as alternating extremely dry periods and intense rainfall events) on landslide occurrence.

## Author contribution

F. Ardizzone, F. Bucci, M. Cardinali, F. Fiorucci, and M. Santangelo mapped in the field the landslides, with the logistic support of O. Althuwaynee, M. Alvioli, T. Bornaetxea, M.T. Brunetti, M. Donnini,

G. Esposito, S.L. Gariano, S. Grita, I. Marchesini, M. Melillo, P. Salvati, and M. Yazdani. M.T. Brunetti, I. Marchesini, M. Melillo, S. Peruccacci, and S.L. Gariano carried out the rainfall analysis. C. Bianchi collected and provided information on fatalities. M. Donnini, M. Santangelo, F. Fiorucci, S.L. Gariano, F. Bucci, and S. Peruccacci wrote the first draft of the paper, revised by all authors. F. Fiorucci coordinated the field survey and the work organization.

## Data availability

Data are available at this repository (Santangelo et al., 2023b) and described in detail in a data description paper (Santangelo et al., 2023a).

## Declarations

**Competing interests** The authors declare no competing interests.

## References

Alvioli M, Mondini AC, Fiorucci F et al (2018) Topography-driven satellite imagery analysis for landslide mapping. Geomat Nat Hazards Risk 9:544–567. https://doi.org/10.1080/19475705.2018.1458050

Antonini G, Ardizzone F, Cardinali M et al (2002) Surface deposits and landslide inventory map of the area affected by the 1997 Umbria-Marche earthquakes. Boll Della Soc Geol Ital Volume spe:843–853

Ardizzone F, Basile G, Cardinali M et al (2012) Landslide inventory map for the Briga and the Giampilieri catchments, NE Sicily, Italy. J Maps 8:176–180. https://doi.org/10.1080/17445647.2012.694271

Avino A, Manfreda S, Cimorelli L, Pianese D (2021) Trend of annual maximum rainfall in Campania region (Southern Italy). Hydrol Process 35. https://doi.org/10.1002/hyp.14447

Bezak N, Mikoš M (2021) Changes in the rainfall event characteristics above the empirical global rainfall thresholds for landslide initiation at the pan-European level. Landslides 18:1859–1873. https://doi.org/10.1007/s10346-020-01579-0

Bornaetxea T, Marchesini I, Kumar S et al (2022) Terrain visibility impact on the preparation of landslide inventories: a practical example in Darjeeling district (India). Nat Hazards Earth Syst Sci 22:2929–2941. https://doi.org/10.5194/nhess-22-2929-2022

Bucci F, Santangelo M, Fongo L, Alvioli M, Cardinali M, Melelli L, Marchesini I (2022) A new digital lithological map of Italy at the 1:100 000 scale for geomechanical modelling. Earth Syst Sci Data 14:4129–4151. https://doi.org/10.5194/essd-14-4129-2022

Buzzi A, Davolio S, Malguzzi P et al (2014) Heavy rainfall episodes over Liguria in autumn 2011: numerical forecasting experiments. Nat Hazards Earth Syst Sci 14:1325–1340. https://doi.org/10.5194/nhess-14-1325-2014

Cardinali M, Ardizzone F, Galli M et al (2000) Landslides triggered by rapid snow melting: the December 1996–January 1997 event in Central Italy. In: Proceedings 1st Plinius conference on Mediterranean storms. Bios, Cosenza, Italy, pp 439–448

Cardinali M, Galli M, Guzzetti F et al (2006) Rainfall induced landslides in December 2004 in south-western Umbria, central Italy: types, extent, damage and risk assessment. Nat Hazards Earth Syst Sci 6:237–260. https://doi.org/10.5194/nhess-6-237-2006

Chiaravalloti F, Caloiero T, Coscarelli R (2022) The long-term ERA5 data series for trend analysis of rainfall in Italy. Hydrology 9:18. https://doi.org/10.3390/hydrology9020018

Corine Land Cover (2021) CORINE land cover product user manual (version 1.0). European Environment Agency (EEA), Kongens Nytorv 6 – 1050 Copenhagen K. – Denmark

Desiato F, Fioravanti G, Fraschetti P et al (2014) Valori climatici normali di temperatura e precipitazione in Italia. ISPRA, Stato dell'Ambiente 55/2014

Desiato F, Lena F, Toreti A (2007) SCIA: a system for a better knowledge of the Italian climate. Boll Geofis Teor Ed Appl 48:351–358

Donnini M, Napolitano E, Salvati P et al (2017) Impact of event landslides on road networks: a statistical analysis of two Italian case studies. Landslides 14:1521–1535. https://doi.org/10.1007/s10346-017-0829-4

Ducrocq V, Braud I, Davolio S et al (2014) HyMeX-SOP1: the field campaign dedicated to heavy precipitation and flash flooding in the northwestern Mediterranean. Bull Am Meteorol Soc 95:1083–1100. https://doi.org/10.1175/BAMS-D-12-00244.1

Duffourg F, Ducrocq V (2011) Origin of the moisture feeding the Heavy Precipitating Systems over Southeastern France. Nat Hazards Earth Syst Sci 11:1163–1178. https://doi.org/10.5194/nhess-11-1163-2011

Esposito E, Porfido S, Simonelli AL et al (2000) Landslides and other surface effects induced by the 1997 Umbria–Marche seismic sequence. Eng Geol 58:353–376. https://doi.org/10.1016/S0013-7952(00)00035-1

Faccini F, Luino F, Paliaga G et al (2018) Role of rainfall intensity and urban sprawl in the 2014 flash flood in Genoa City, Bisagno catchment (Liguria, Italy). Appl Geogr 98:224–241. https://doi.org/10.1016/j.apgeog.2018.07.022

Fiori E, Comellas A, Molini L et al (2014) Analysis and hindcast simulations of an extreme rainfall event in the Mediterranean area: the Genoa 2011 case. Atmospheric Res 138:13–29. https://doi.org/10.1016/j.atmosres.2013.10.007

Fiorucci F, Cardinali M, Carlà R et al (2011) Seasonal landslide mapping and estimation of landslide mobilization rates using aerial and satellite images. Geomorphology 129:59–70. https://doi.org/10.1016/j.geomorph.2011.01.013

Floris M, Veneri F (2004) Landslide risk assessment in Italy: a case study in the Umbria-Marche Apennines. In: Hack R, Azzam R, Charlier R (eds) Engineering Geology for Infrastructure Planning in Europe: A European Perspective. Springer, Berlin, Heidelberg, pp 738–744

Fratianni S, Acquaotta F (2017) The climate of Italy. In: Soldati M, Marchetti M (eds) Landscapes and landforms of Italy. Springer International Publishing, Cham, pp 29–38

Froude MJ, Petley DN (2018) Global fatal landslide occurrence from 2004 to 2016. Nat Hazards Earth Syst Sci 18:2161–2181. https://doi.org/10.5194/nhess-18-2161-2018

Gariano SL, Guzzetti F (2016) Landslides in a changing climate. Earth Sci Rev 162:227–252. https://doi.org/10.1016/j.earscirev.2016.08.011

Gariano SL, Verini Supplizi G, Ardizzone F et al (2021) Long-term analysis of rainfall-induced landslides in Umbria, central Italy. Nat Hazards 106:2207–2225. https://doi.org/10.1007/s11069-021-04539-6

Guzzetti F (2000) Landslide fatalities and the evaluation of landslide risk in Italy. Eng Geol 58:89–107. https://doi.org/10.1016/S0013-7952(00)00047-8

Guzzetti F, Malamud BD, Turcotte DL, Reichenbach P (2002) Power-law correlations of landslide areas in central Italy. Earth Planet Sci Lett 195:169–183. https://doi.org/10.1016/S0012-821X(01)00589-1

Guzzetti F, Mondini AC, Cardinali M et al (2012) Landslide inventory maps: new tools for an old problem. Earth Sci Rev 112:42–66. https://doi.org/10.1016/j.earscirev.2012.02.001

Guzzetti F, Reichenbach P, Cardinali M et al (2003) The impact of landslides in the Umbria region, central Italy. Nat Hazards Earth Syst Sci 3:469–486. https://doi.org/10.5194/nhess-3-469-2003

Guzzetti F, Stark CP, Salvati P (2005) Evaluation of flood and landslide risk to the population of Italy. Environ Manag 36:15–36. https://doi.org/10.1007/s00267-003-0257-1

Haque U, da Silva PF, Devoli G et al (2019) The human cost of global warming: deadly landslides and their triggers (1995–2014). Sci Total Environ 682:673–684. https://doi.org/10.1016/j.scitotenv.2019.03.415

Herath S, Wang Y (2009) Case studies and national experiences. In: Sassa K, Canuti P (eds) Landslides – disaster risk reduction. Springer, Berlin, Heidelberg, pp 475–497

Hungr O, Leroueil S, Picarelli L (2014) The Varnes classification of landslide types, an update. Landslides 11:167–194. https://doi.org/10.1007/s10346-013-0436-y

Liang X, Segoni S, Yin K, Du J, Chai B, Tofani V, Casagli N (2022) Characteristics of landslides and debris flows triggered by extreme rainfall in Daoshi Town during the 2019 Typhoon Lekima, Zhejiang Province, China. Landslides 19:1735–1749. https://doi.org/10.1007/s10346-022-01889-5

Libertino A, Ganora D, Claps P (2019) Evidence for increasing rainfall extremes remains elusive at large spatial scales: the case of Italy. Geophys Res Lett 46:7437–7446. https://doi.org/10.1029/2019GL083371

Malamud BD, Turcotte DL, Guzzetti F, Reichenbach P (2004) Landslide inventories and their statistical properties. Earth Surf Process Landf 29:687–711. https://doi.org/10.1002/esp.1064

Mazzoglio P, Butera I, Alvioli M, Claps P (2022) The role of morphology in the spatial distribution of short-duration rainfall extremes in Italy. Hydrol Earth Syst Sci 26:1659–1672. https://doi.org/10.5194/hess-26-1659-2022

Mirabella F, Bucci F, Santangelo M et al (2018) Alluvial fan shifts and stream captures driven by extensional tectonics in central Italy. J Geol Soc 175:788–805. https://doi.org/10.1144/jgs2017-138

Mondini AC, Viero A, Cavalli M et al (2014) Comparison of event landslide inventories: the Pogliaschina catchment test case, Italy. Nat Hazards Earth Syst Sci 14:1749–1759. https://doi.org/10.5194/nhess-14-1749-2014

Nuissier O, Ducrocq V, Ricard D et al (2008) A numerical study of three catastrophic precipitating events over southern France. I: Numerical framework and synoptic ingredients. Q J R Meteorol Soc 134:111–130. https://doi.org/10.1002/qj.200

Pensieri S, Schiano M, Picco P et al (2018) Analysis of the precipitation regime over the Ligurian Sea. Water 10:566. https://doi.org/10.3390/w10050566

Pereira S, Zêzere JL, Quaresma I et al (2016) Mortality patterns of hydro-geomorphologic disasters: mortality patterns of hydro-geomorphologic disasters. Risk Anal 36:1188–1210. https://doi.org/10.1111/risa.12516

Peruccacci S, Brunetti MT, Luciani S et al (2012) Lithological and seasonal control on rainfall thresholds for the possible initiation of landslides in central Italy. Geomorphology 139–140:79–90. https://doi.org/10.1016/j.geomorph.2011.10.005

Petley D (2012) Global patterns of loss of life from landslides. Geology 40:927–930. https://doi.org/10.1130/G33217.1

Polaris (2022) Rapporto Periodico sul Rischio posto alla Popolazione Italiana da Frane e da Inondazioni - Anno 2022. https://polaris.irpi.cnr.it/report/last-report/. Accessed 21 June 2023

Regione Marche - Centro Funzionale Regionale (2022) Rapporto di evento preliminare Maltempo 15,16 e 17 Settembre 2022. In Italian

Reichenbach P, Rossi M, Malamud BD et al (2018) A review of statistically-based landslide susceptibility models. Earth-Sci Rev 180:60–91. https://doi.org/10.1016/j.earscirev.2018.03.001

Ricciardelli E, Cersosimo A, Cimini D et al (2018) Analysis of heavy rainfall events occurred in Italy by using numerical weather prediction, microwave and infrared technique. In: IGARSS 2018 - 2018 IEEE International Geoscience and Remote Sensing Symposium. IEEE, Valencia, pp 931–934

Salvati P, Bianchi C, Rossi M, Guzzetti F (2010) Societal landslide and flood risk in Italy. Nat Hazards Earth Syst Sci 10:465–483. https://doi.org/10.5194/nhess-10-465-2010

Salvati P, Pernice U, Bianchi C et al (2016) Communication strategies to address geohydrological risks: the POLARIS web initiative in Italy. Nat Hazards Earth Syst Sci 16:1487–1497. https://doi.org/10.5194/nhess-16-1487-2016

Salvati P, Petrucci O, Rossi M et al (2018) Gender, age and circumstances analysis of flood and landslide fatalities in Italy. Sci Total Environ 610–611:867–879. https://doi.org/10.1016/j.scitotenv.2017.08.064

Santangelo M, Marchesini I, Bucci F et al (2021) Exposure to landslides in rural areas in Central Italy. J Maps 17:124–132. https://doi.org/10.1080/17445647.2020.1746699

Santangelo M, Cardinali M, Bucci F et al (2022) Exploring event landslide mapping using Sentinel-1 SAR backscatter products. Geomorphology 397:108021. https://doi.org/10.1016/j.geomorph.2021.108021

Santangelo M, Althuwaynee O, Alvioli M, Ardizzone F, Bianchi C, Bornaetxea T, Brunetti MT, Bucci F, Cardinali M, Donnini M, Esposito G, Gariano SL, Grita S, Marchesini I, Melillo M, Peruccacci S, Salvati P, Yazdani M, Fiorucci F (2023a) Inventory of landslides triggered by an extreme rainfall event in Marche-Umbria, Italy, on 15 September 2022. Scientific Data. https://doi.org/10.1038/s41597-023-02336-3

Santangelo M, Althuwaynee O, Alvioli M, Ardizzone F, Bianchi C, Bornaetxea T, Brunetti MT, Bucci F, Cardinali M, Donnini M, Esposito G, Gariano SL, Grita S, Marchesini I, Melillo M, Peruccacci S, Salvati P, Yazdani M, Fiorucci F (2023b) Inventory of landslides triggered by anextreme rainfall event in Marche-Umbria, Italy, on 15 September 2022. Figshare. Dataset. https://doi.org/10.6084/m9.figshare.21981842.v1

Scofield RA (1985) Satellite convective categories associated with heavy precipitation. In: Preprints for Sixth Conf. on Hydrometeorology. Amer Meteor Soc pp 42–51

Westra S, Fowler HJ, Evans JP et al (2014) Future changes to the intensity and frequency of short-duration extreme rainfall: future intensity of sub-daily rainfall. Rev Geophys 52:522–555. https://doi.org/10.1002/2014RG000464

**Marco Donnini · Michele Santangelo (✉) ·**
**Stefano Luigi Gariano · Francesco Bucci · Silvia Peruccacci**
**· Massimiliano Alvioli · Omar Althuwaynee ·**
**Francesca Ardizzone · Cinzia Bianchi · Maria Teresa Brunetti**
**· Mauro Cardinali · Giuseppe Esposito · Susanna Grita**
**· Ivan Marchesini · Massimo Melillo · Paola Salvati ·**
**Mina Yazdani · Federica Fiorucci**
Italian National Research Council - Research Institute
for Geo-Hydrological Protection (CNR-IRPI), Perugia, Italy
Email: michele.santangelo@irpi.cnr.it

**Txomin Bornaetxea**
Universidad del País Vasco/Euskal Herriko Unibertsitatea (UPV/EHU),
Leioa, Spain

**Susanna Grita**
Università degli Studi di Roma "La Sapienza", Rome, Italy